

Optical and generation characteristics of new nonlinear $\text{Ba}_2\text{Ga}_8\text{GeS}_{16}$ and $\text{Ba}_2\text{Ga}_8(\text{GeSe}_2)\text{S}_{14}$ crystals for the mid-IR range

V.V. Badikov, D.V. Badikov, G.S. Shevyrdyaeva, V.B. Laptev, A.A. Melnikov, S.V. Chekalin

Abstract. $\text{Ba}_2\text{Ga}_8\text{GeS}_{16}$ and $\text{Ba}_2\text{Ga}_8(\text{GeSe}_2)\text{S}_{14}$ single crystals of large size and good optical quality have been grown for the first time. Their linear optical characteristics—transmission spectra in the range of 0.3–25 μm , dispersion of principal refractive indices, and birefringence—have been measured. Irradiation of the crystals by 100-fs laser pulses with a wavelength of 8.3 μm initiated second-harmonic generation with an efficiency comparable with that obtained for the AgGaS_2 crystal.

Keywords: nonlinear optical crystals, second harmonic generation.

1. Introduction

Nonlinear optical crystals are widely used in modern laser systems. These crystals make it possible to extend significantly the frequency range due to the generation of sum and difference frequencies, as well as optical parametric generation. Since mid-IR laser radiation has many important applications in science, technology, and medicine, much attention is paid to the synthesis of new high-efficiency nonlinear crystals for this spectral region.

Since the beginning of the 2000s, several dozens of new crystals for the mid-IR range have been synthesised [1, 2]; however, only few of them are currently commercially available and widely used due to their good characteristics. Primarily, these are nonlinear crystals AgGaS_2 , AgGaSe_2 , and ZnGeP_2 , which are applied for frequency doubling of pulsed CO_2 lasers and for parametric generation with pumping by Nd and Yb lasers at a wavelength of $\sim 1 \mu\text{m}$ and Er laser at a wavelength of $\sim 1.5 \mu\text{m}$. These crystals are characterised by a high quadratic nonlinear susceptibility, a low absorbance at frequencies of interacting waves, and a sufficiently high mechanical strength [1]. At the same time, as was noted by some researchers, many of nonlinear crystals similar to the aforementioned ones have a low damage threshold (several J cm^{-2} and several tens of MW cm^{-2}) for nanosecond IR laser radiation (see, e. g., [1, 2] and references therein).

V.V. Badikov, D.V. Badikov, G.S. Shevyrdyaeva Kuban State University, ul. Stavropol'skaya 149, 350040 Krasnodar, Russia; e-mail: badikov@list.ru, badikovd@gmail.com, galinashevyrdyaeva@gmail.com;

V.B. Laptev, A.A. Melnikov, S.V. Chekalin Institute of Spectroscopy, Russian Academy of Sciences, ul. Fizicheskaya 5, 108840 Troitsk, Moscow, Russia; e-mail: laptev@isan.troitsk.ru, melnikov@isan.troitsk.ru, chekalin@isan.troitsk.ru

Received 26 October 2021; revision received 7 December 2021
Kvantovaya Elektronika 52 (3) 296–300 (2022)
Translated by Yu.P. Sin'kov

A relatively short time ago researchers became interested in quaternary barium chalcogenide crystals of the BaGa_2AB_6 type ($A = \text{Si, Ge}$; $B = \text{S, Se}$) [3–7]. Crystals of this type possess simultaneously high nonlinear susceptibility and high radiation resistance. Our measurements [7] showed the surface damage thresholds for $\text{BaGa}_2\text{GeS}_6$ and $\text{BaGa}_2\text{GeSe}_6$ single crystals, irradiated by single CO_2 laser pulses with a duration of $\sim 100 \text{ ns}$ and a wavelength of 10.6 μm , to be, respectively, 14 J cm^{-2} (140 MW cm^{-2}) and 11 J cm^{-2} (110 MW cm^{-2}).

Liu et al. [8] reported about synthesis of polycrystalline samples of two new metal sulfides $\text{Ba}_2\text{Ga}_8\text{MS}_{16}$ ($M = \text{Si, Ge}$) with wide band gaps: 3.4 and 3.0 eV, respectively. The $\text{Ba}_2\text{Ga}_8\text{GeS}_{16}$ sample made it possible to implement second-harmonic generation (SHG) with efficiency comparable to that obtained for AgGaS_2 crystals; at the same time, the threshold radiation resistance of $\text{Ba}_2\text{Ga}_8\text{GeS}_{16}$ irradiated by 8-ns laser pulses with a wavelength of 1.064 μm was 22 times higher than that of AgGaS_2 .

The objects of our study are $\text{Ba}_2\text{Ga}_8\text{GeS}_{16}$ and $\text{Ba}_2\text{Ga}_8(\text{GeSe}_2)\text{S}_{14}$ single crystals of large size and good optical quality; these crystals have been grown for the first time. We have measured their transmission spectra in the UV, visible, and mid-IR ranges (0.3–25 μm); dispersion of the principal refractive indices; and birefringence. The band gaps of $\text{Ba}_2\text{Ga}_8\text{GeS}_{16}$ and $\text{Ba}_2\text{Ga}_8(\text{GeSe}_2)\text{S}_{14}$ crystals were 3.07 and 2.65 eV, respectively. SHG with efficiency comparable to that for AgGaS_2 was obtained when irradiating these ternary crystals by 100-fs laser pulses at a wavelength of 8.3 μm .

2. Growth of $\text{Ba}_2\text{Ga}_8\text{GeS}_{16}$ and $\text{Ba}_2\text{Ga}_8(\text{GeSe}_2)\text{S}_{14}$ single crystals and their crystallographic properties

New nonlinear crystals $\text{Ba}_2\text{Ga}_8\text{GeS}_{16}$ and $\text{Ba}_2\text{Ga}_8(\text{GeSe}_2)\text{S}_{14}$ were successfully grown by the Bridgman–Stockbarger technique in vertical growth systems. Using chemical elements Ba (99.99%), Ga (99.999%), Ge (99.999%), S, and Se (99.999%), we synthesised binary compounds Ga_2S_3 , GeSe_2 , and GeS_2 in quartz ampoules (previously evacuated to a pressure of 10^{-6} mbar) at a high temperature, with subsequent annealing for melt homogenisation. $\text{Ba}_2\text{Ga}_8\text{GeS}_{16}$ and $\text{Ba}_2\text{Ga}_8(\text{GeSe}_2)\text{S}_{14}$ crystals were synthesised in graphitised quartz ampoules, filled with metallic barium and sulfur (BaS composition) and Ga_2S_3 , GeSe_2 , and GeS_2 compounds in ratios corresponding to the composition chemical formulas. Ampoules, evacuated previously to 10^{-6} mbar, were sealed using a gas burner, placed in a horizontal furnace to perform synthesis, and heated to 1050 $^\circ\text{C}$ for 12 h. The melts obtained were kept at this temperature for 24 h and stirred for complete homogeni-

sation. Growth was performed in vertical furnaces with a temperature gradient of $10\text{--}15^\circ\text{C cm}^{-1}$ in the crystallisation zone, with melt heated to a temperature exceeding the melting point by $30\text{--}40^\circ\text{C}$. Both compositions had a congruent character of melting. The melting points for the $\text{Ba}_2\text{Ga}_8\text{GeS}_{16}$ and $\text{Ba}_2\text{Ga}_8(\text{GeSe}_2)\text{S}_{14}$ compositions were, respectively, 1008 and 994°C . The crystal growth rate was 6 mm per day . The grown crystals were cooled to room temperature with the switched-off furnace. The $\text{Ba}_2\text{Ga}_8\text{GeS}_{16}$ single crystals were colourless. The photograph in Fig. 1 shows a grown-sample fragment.

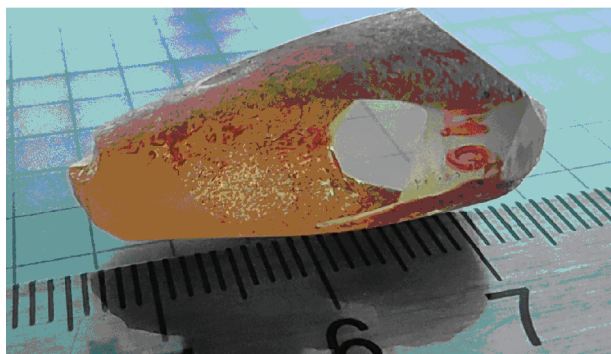
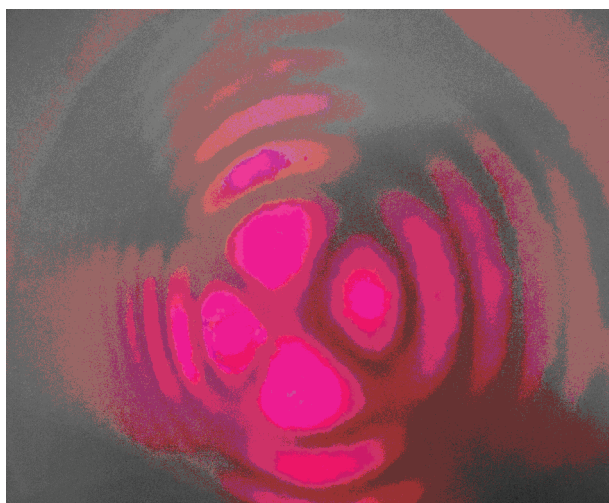


Figure 1. (Colour online) Photograph of the $\text{Ba}_2\text{Ga}_8\text{GeS}_{16}$ crystal.

The crystals belong to the point symmetry group C_{6v} (6mm) and are crystallised in the noncentrosymmetric space group $P6_3mc$ with the lattice parameters $a = 10.8826\text{ \AA}$ and $c = 11.9017\text{ \AA}$.

The crystal samples were preliminarily oriented using conoscopy. Figure 2 shows conoscopic images, recorded in monochromatic light on plates (cut from uniaxial crystals) installed between two crossed polarisers. Light propagated along the principal crystallographic axis (Fig. 2a) and perpendicular to it (Fig. 2b). In the final stage the crystalline samples were oriented using an X-ray diffractometer DRON-2.0.



a

3. Transmission spectra and dispersion relations

The transmission spectra of 0.51-mm-thick $\text{Ba}_2\text{Ga}_8\text{GeS}_{16}$ and $\text{Ba}_2\text{Ga}_8(\text{GeSe}_2)\text{S}_{14}$ single crystals in the UV, visible, and near-IR ($0.3\text{--}1\text{ }\mu\text{m}$) and mid-IR ($2.5\text{--}25\text{ }\mu\text{m}$) ranges were measured in unpolarised light at room temperature using Specord 250 (Analytic Jena) and Specord M82 (Carl Zeiss Jena) spectrophotometers. The spectra are presented in Fig. 3, along with the photographs of crystal samples placed on a millimetre grid.

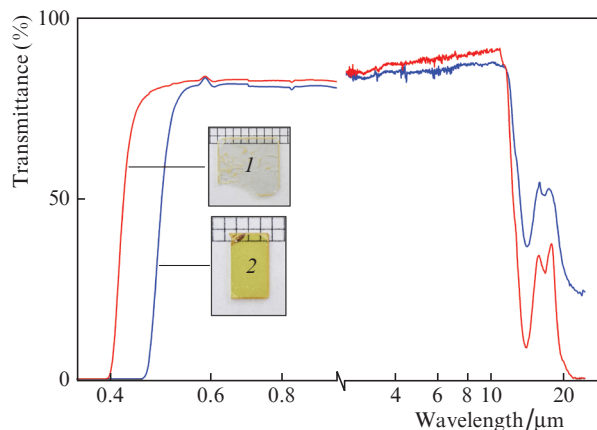
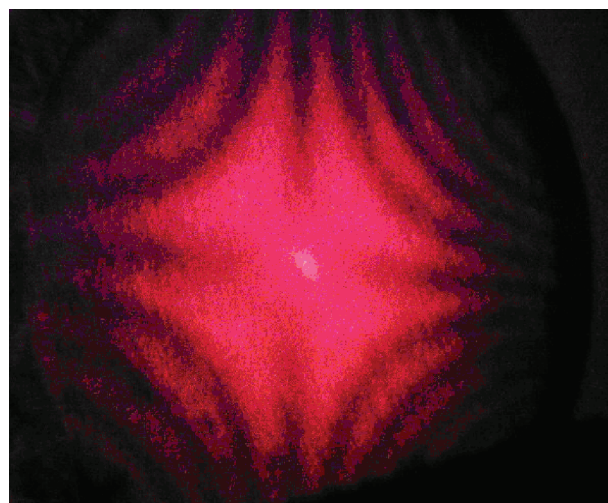


Figure 3. (Colour online) Transmission spectra of 0.51-mm-thick (1) $\text{Ba}_2\text{Ga}_8\text{GeS}_{16}$ and (2) $\text{Ba}_2\text{Ga}_8(\text{GeSe}_2)\text{S}_{14}$ single crystals. Measurements were performed in unpolarised light at room temperature. The sample photographs are shown in the insets.

$\text{Ba}_2\text{Ga}_8\text{GeS}_{16}$ and $\text{Ba}_2\text{Ga}_8(\text{GeSe}_2)\text{S}_{14}$ crystals are transparent in the spectral ranges of $0.48\text{--}11.8\text{ }\mu\text{m}$ and $0.53\text{--}11.9\text{ }\mu\text{m}$. Zero transmission of $\text{Ba}_2\text{Ga}_8\text{GeS}_{16}$ and $\text{Ba}_2\text{Ga}_8(\text{GeSe}_2)\text{S}_{14}$ crystals from the side of visible range is observed at wavelengths of 0.407 and $0.465\text{ }\mu\text{m}$, respectively. This circumstance makes it possible to estimate the room-temperature band



b

Figure 2. (Colour online) Conoscopy of the $\text{Ba}_2\text{Ga}_8\text{GeS}_{16}$ crystal along the (a) Z and (b) Y axes.

gaps for the samples as 3.07 and 2.67 eV. The value of 3.07 eV for the $\text{Ba}_2\text{Ga}_8\text{GeS}_{16}$ single crystal correlates well with the value of 3.0 eV, found in [8] for a polycrystalline sample from diffuse reflection spectra. High transparency of both crystals is observed in the mid-IR range up to $\sim 12 \mu\text{m}$, after which it gradually decreases to zero at a wavelength of $\sim 21.3 \mu\text{m}$ for $\text{Ba}_2\text{Ga}_8\text{GeS}_{16}$, whereas the $\text{Ba}_2\text{Ga}_8(\text{GeSe}_2)\text{S}_{14}$ crystal retains nonzero transparency (25%) up to $25 \mu\text{m}$.

The dependences of the dispersion of principal refractive indices n_o and n_e for the $\text{Ba}_2\text{Ga}_8\text{GeS}_{16}$ single crystal were measured on a bench designed at the Kuban State University, which is intended to measure refractive indices of prisms with refracting faces about $5 \times 5 \text{ mm}$ in size [9].

Measurements were performed in three spectral ranges (using different methods in each):

(i) visible range (the least deviation method in the range of $0.4\text{--}0.6 \mu\text{m}$), with the aid of a GS-2 spectrometer-goniometer, a mercury lamp, and a sodium lamp;

(ii) visible and near-IR ranges: $0.4\text{--}1.8 \mu\text{m}$ (autocollimation method), using a GS-2 goniometer, an MDR-2 monochromator, a halogen incandescent lamp, a collimating objective, and a photodetection unit with a germanium photodiode;

(iii) mid-IR range: $2.0\text{--}10 \mu\text{m}$ (autocollimation method), using a GS-2 goniometer, an IKS-21 monochromator, a globar, a collimating objective, and a photodetection unit with a pyroelectric element. The measurement error was 5×10^{-4} in the range of $0.5\text{--}1.2 \mu\text{m}$ and 10^{-3} for $2\text{--}12 \mu\text{m}$.

The dispersion of the principal refractive indices of the $\text{Ba}_2\text{Ga}_8\text{GeS}_{16}$ single crystal was measured in the spectral range of $0.546\text{--}10.0 \mu\text{m}$ using a prism (Fig. 4) with a refractive angle of $14^\circ 00' 08''$ and face aperture of $14.2 \times 12.4 \text{ mm}$. The found values of refractive indices for the $\text{Ba}_2\text{Ga}_8\text{GeS}_{16}$ crystal are given in Table 1 and Fig. 5.

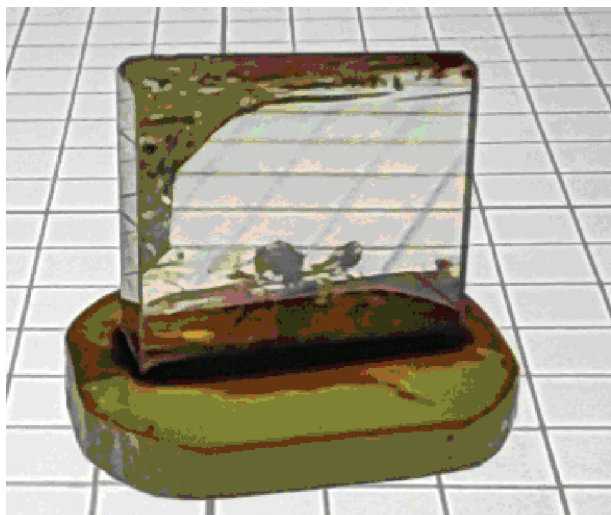


Figure 4. (Colour online) Prism made of the $\text{Ba}_2\text{Ga}_8\text{GeS}_{16}$ crystal.

To calculate the phase-matching angles, we approximated the experimental dependences of the principal refractive indices n_o and n_e on wavelength λ in the transparency range by a function in the form of (Sellmeier equation)

$$n^2 = A_1 + \frac{A_3}{\lambda^2 - A_2} + \frac{A_5}{\lambda^2 - A_4}. \quad (1)$$

Table 1. Experimental dependences of principal refractive indices n_o , n_e on the radiation wavelength.

Wave-length / μm	n_o	n_e	Δn	Wave-length / μm	n_o	n_e	Δn
0.546	2.437	2.396	0.041	2.0	2.305	2.272	0.033
0.578	2.419	2.379	0.040	3.0	2.300	2.265	0.035
0.7	2.380	2.342	0.038	4.0	2.294	2.261	0.033
0.9	2.341	2.308	0.032	5.0	2.288	2.253	0.035
1.1	2.326	2.292	0.032	6.0	2.280	2.247	0.033
1.3	2.316	2.284	0.032	7.0	2.272	2.238	0.034
1.5	2.311	2.278	0.033	8.0	2.261	2.232	0.029
1.7	2.307	2.278	0.032	9.0	2.252	2.225	0.027
1.8	2.306	2.273	0.033	10.0	2.245	2.218	0.027

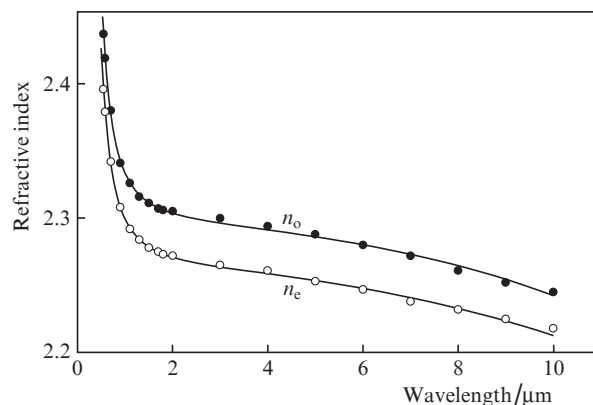


Figure 5. Measured (circles) and calculated (solid lines) dependences of the principal refractive indices n_o and n_e on the light wavelength for the $\text{Ba}_2\text{Ga}_8\text{GeS}_{16}$ crystal.

The Sellmeier coefficients found by fitting are listed in Table 2. The calculated wavelength dependences of the refractive indices n_o and n_e for the $\text{Ba}_2\text{Ga}_8\text{GeS}_{16}$ crystal are presented in Fig. 5 (solid lines). The Sellmeier equations for the refractive indices n_o and n_e made it possible to calculate the dependence of the phase-matching angle on the fundamental radiation wavelength for the first-type SHG (oo-e process) (Fig. 6).

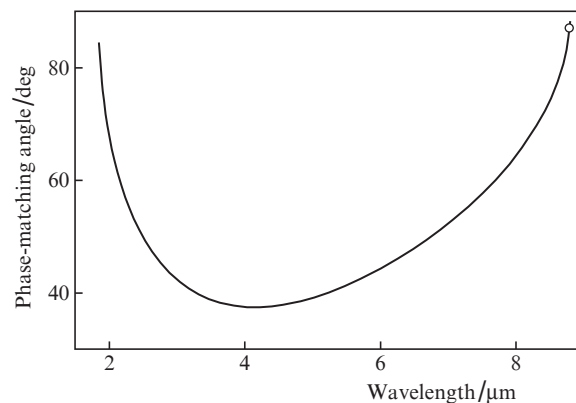


Figure 6. Calculated dependence of the phase-matching angle for SHG (oo-e process) on the fundamental radiation wavelength for the $\text{Ba}_2\text{Ga}_8\text{GeS}_{16}$ crystal. The circle on the curve indicates the phase-matching angle for sample No. 1 with the phase-matching angle $\theta = 87^\circ$ and wavelength $8.8 \mu\text{m}$.

Table 2. Sellmeier coefficients.

Crystal	n	A_1	A_2 / μm^2	A_3 / μm^2	A_4 / μm^2	A_5 / μm^2
$\text{Ba}_2\text{Ga}_8\text{GeS}_{16}$ (transmission range from 0.55 to 10.0 μm)	n_o	6.477	0.048	0.164	588	708
	n_e	7.43	0.0506	0.152	1092.0	2516

4. Second harmonic generation in $\text{Ba}_2\text{Ga}_8\text{GeS}_{16}$ and $\text{Ba}_2\text{Ga}_8(\text{GeSe}_2)\text{S}_{14}$ crystals

Pulsed mid-IR radiation was used as fundamental to obtain SHG in the $\text{Ba}_2\text{Ga}_8\text{GeS}_{16}$ and $\text{Ba}_2\text{Ga}_8(\text{GeSe}_2)\text{S}_{14}$ crystal samples under study; the radiation source was a femtosecond system (the Collective Use Centre of the Institute of Spectroscopy, RAS). It consists of a master Ti:sapphire oscillator Tsunami (Spectra-Physics, United States), which served as a pump source for a regenerative amplifier Spitfire HP; the latter generated 800-nm pulses with a duration of 50 fs and energy of 1.2 mJ. Then this radiation was supplied at the input of parametric amplifier TOPAS-C. The signal and idler waves from its output were supplied at a difference-frequency generator NDFG (Light Conversion, Lithuania) based on an AgGaS_2 crystal. The repetitively pulsed radiation at the generator output had the following parameters: pulse repetition rate of 1 kHz, pulse energy of $7.2 \pm 0.2 \mu\text{J}$, pulse duration of ~ 100 fs, centre wavelength of 8.3 μm , and spectral FWHM of $\sim 230 \text{ cm}^{-1}$. The radiation was focused on the surface of crystals under study by a gold spherical mirror with a focal length of 20 cm.

The transverse and longitudinal distributions of laser beam energy at the fundamental wavelength were measured using a pyroelectric matrix Pyrocam III (Spiricon Inc., USA). The beam caustic length was about 4 mm, and the focused spot had an elliptical shape with axis lengths of 130 and 150 μm . Thus, the radiation incident on the crystal surface had an energy density of 47 mJ cm^{-2} and an intensity of $4.7 \times 10^{11} \text{ W cm}^{-2}$ in a pulse. To cut off the fundamental-wavelength radiation (at 8.3 μm) from the second harmonic, the laser beam transmitted through the nonlinear crystal was passed through a 5-mm-thick sapphire plate. The power of filtered second-harmonic beam was measured by a bolometer.

Experiments were performed with samples of nonlinear $\text{Ba}_2\text{Ga}_8\text{GeS}_{16}$ (Nos 1 and 2) and $\text{Ba}_2\text{Ga}_8(\text{GeSe}_2)\text{S}_{14}$ crystals. Each crystal had a thickness of 0.51 mm, and the phase-matching angle θ relative to the optical axis Z , equal to 87° ($\varphi = 30^\circ$), corresponded to the fundamental radiation wavelength (8.8 μm). However, because of certain technical limitations, we chose the fundamental radiation wavelength to be 8.3 μm . This deviation affected only slightly the SHG process because of the wide radiation spectrum of femtosecond pulses. The first-type SHG process (oo-e) was investigated. To obtain SHG tuning curves, the crystals were rotated around the axis parallel to the fundamental-beam polarisation vector in the range of ± 40 – 50° . The fundamental and second-harmonic radiation spectra were measured using a grating monochromator and a pyroelectric detector, installed behind its output slit. The SHG efficiency in the crystals studied was compared with that for a reference AgGaS_2 crystal of the same thickness (0.51 mm). The AgGaS_2 crystal had a phase-matching angle $\theta = 48.5^\circ$ ($\varphi = 45^\circ$), a value appropriate for SHG at the fundamental radiation wavelength of 8.3 μm .

The spectra of the fundamental and second harmonic radiation, recorded in our experiments for $\text{Ba}_2\text{Ga}_8\text{GeS}_{16}$ crystal No. 2, are presented in Fig. 7. The former had a pronounced dip near its centre wavelength, which is independent of the presence or absence of crystal studied on the radiation path to the monochromator input slit. Successive recording of fundamental radiation spectrum showed that the dip depth changes from a rather small value to that shown in Fig. 7. The occurrence of spectral dip is apparently due to the specific features of generating radiation with the central wavelength of 8.3 μm , because, when the latter decreases to about 8 μm , the dip virtually disappears and the spectrum becomes smoother. Nevertheless, the spectral dependence presented in Fig. 7 demonstrates clearly the appearance of a second-harmonic peak at $\sim 4.2 \mu\text{m}$.

The dependences of the second-harmonic pulse energy on the external angle of incidence of radiation at the fundamental wavelength of 8.3 μm for $\text{Ba}_2\text{Ga}_8\text{GeS}_{16}$, $\text{Ba}_2\text{Ga}_8(\text{GeSe}_2)\text{S}_{14}$, and AgGaS_2 crystals (Fig. 8) demonstrate that crystal rotation only slightly changes the second-harmonic pulse energy, despite a significant (± 40 – 50°) change in the angle of laser

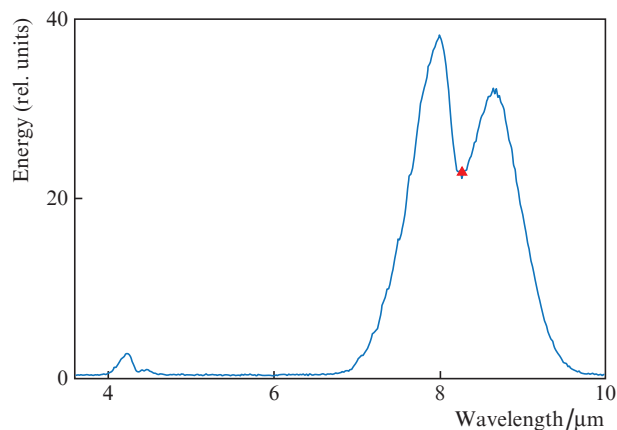


Figure 7. (Colour online) Radiation spectra of the fundamental and second harmonic for $\text{Ba}_2\text{Ga}_8\text{GeS}_{16}$ crystal No. 2. The centre wavelength (8.3 μm) is indicated by a red triangle.

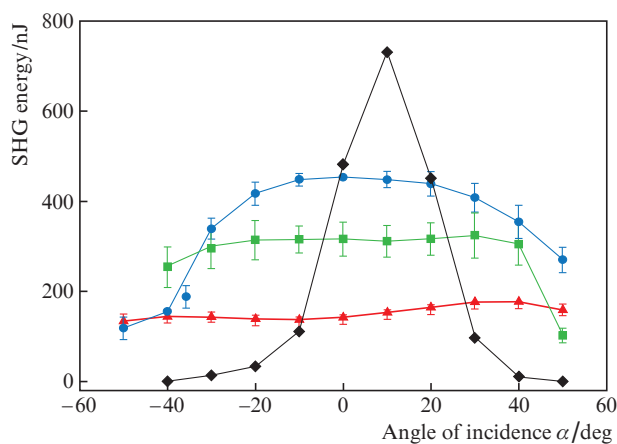


Figure 8. (Colour online) Measured dependences of the second-harmonic pulse energy on the external angle of incidence α of fundamental radiation for $\text{Ba}_2\text{Ga}_8\text{GeS}_{16}$ crystals No. 1 (circles) and No. 2 (squares), $\text{Ba}_2\text{Ga}_8(\text{GeSe}_2)\text{S}_{14}$ crystal (triangles), and reference AgGaS_2 crystal (diamonds).

beam incidence. This behaviour of the SHG tuning curve can be explained by realisation of a phase-matching angle non-critical regime, when the difference in the angular derivatives for refractive indices is close to zero [10]. This fact is an indirect manifestation of the sharp dependence of phase-matching angle on the radiation wavelength in the range of 8–8.8 μm (see Fig. 6). As a result, the fundamental radiation spectral width (FWHM $\sim 1.5 \mu\text{m}$) overlaps completely the entire range of phase-matching angles corresponding to the external angle of incidence of the beam (± 40 – 50°), and the crystal rotation leads only to a small variation in the second-harmonic pulse energy.

We did not perform any special experiments aimed at measuring laser damage thresholds for $\text{Ba}_2\text{Ga}_8\text{GeS}_{16}$ and $\text{Ba}_2\text{Ga}_8(\text{GeSe}_2)\text{S}_{14}$ crystals irradiated by femtosecond pulses. Nevertheless, it should be noted that, when recording the tuning characteristics, we did not observe any (even insignificant) damage of the crystal surface, despite the fact that the radiation intensity was $4.7 \times 10^{11} \text{ W cm}^{-2}$, and the total number of pulses was as high as 10^6 – 10^7 . Thus, one can suggest that the threshold laser damage intensity for the crystals under consideration, irradiated by 100-fs pulses at a wavelength of 8.3 μm , obviously exceeds $5 \times 10^{11} \text{ W cm}^{-2}$.

5. Conclusions

The main results of this study are as follows: $\text{Ba}_2\text{Ga}_8\text{GeS}_{16}$ and $\text{Ba}_2\text{Ga}_8(\text{GeSe}_2)\text{S}_{14}$ single crystals of high optical quality and $\sim 1 \text{ cm}$ in size were grown for the first time by the Bridgman–Stockbarger method. Their transmission spectra in the ranges of 0.3–1 and 2.5–25 μm , the dispersion relations for principal refractive indices, and the birefringence were measured. The crystals are transparent in the spectral ranges of 0.48–11.8 and 0.53–11.9 μm . The band gaps of the $\text{Ba}_2\text{Ga}_8\text{GeS}_{16}$ and $\text{Ba}_2\text{Ga}_8(\text{GeSe}_2)\text{S}_{14}$ crystals are 3.07 and 2.65 eV, respectively. SHG was obtained in these crystals under irradiation by a 100-fs laser beam with a fundamental wavelength of 8.3 μm . The SHG tuning characteristics were measured for two samples of the $\text{Ba}_2\text{Ga}_8\text{GeS}_{16}$ crystal and one sample of the $\text{Ba}_2\text{Ga}_8(\text{GeSe}_2)\text{S}_{14}$ crystal. The SHG efficiency of these crystals turned out to be comparable with that of the AgGaS_2 crystal.

References

1. Nikogosyan D.N. *Nonlinear Optical Crystals: A Complete Survey* (New York: Springer, 2005).
2. Petrov V. *Progr. Quantum Electron.*, **42**, 1 (2015).
3. Lin X., Guo Y., Ye N., Zhai N. *J. Solid State Chem.*, **195**, 172 (2012).
4. Yin W., Feng K., He R., Mei D., Lin Z., Yao J., Wu Y. *Dalton Trans.*, **41**, 5653 (2012).
5. Grechin S.G., Nikolaev P.P., Ionin A.A., Kinyaevskii I.O., Andreev Yu.M. *Quantum Electron.*, **50**, 782 (2020) [*Kvantovaya Elektron.*, **50**, 782 (2020)].
6. Petrov V., Badikov V.V., Badikov D.V., Kato K., Shevyrdyaeva G.S., Miyata K., Mero M., Wang Li, Heiner Z., Panyutin V.L. *J. Opt. Soc. Am. B*, **38**, B46 (2021).
7. Badikov V.V., Badikov D.V., Laptev V.B., Mitin K.V., Shevyrdyaeva G.S., Shchebetova N.I., Petrov V. *Opt. Mater. Express*, **6**, 2933 (2016).
8. Liu B., Zeng H., Zhang M., Fan Y., Guo G., Huang J., Dong Z. *Inorg. Chem.*, **54**, 976 (2015).
9. Zlochik I.Kh. *Opticheskie svoystva i usloviya rosta tiogallatov serebra i rtuti* (Optical Properties and Conditions for Growth of Silver and Mercury Thiogallates). Ed. by N.D. Ustinov (Moscow: VINITI, 1982).
10. Grechin S.G., Dmitriev V.G., D'yakov V.A., Pryalkin V.I. *Quantum Electron.*, **28**, 937 (1998) [*Kvantovaya Elektron.*, **25**, 963 (1998)].